Progress in Organic Coatings 163 (2022) 106614

Contents lists available at ScienceDirect

Progress in Organic Coatings

journal homepage: www.elsevier.com/locate/porgcoat

The effect of mechanical and thermal stresses on the performance of lubricated icephobic coatings during cyclic icing/deicing tests

Valentina Donadei *, Heli Koivuluoto, Essi Sarlin, Henna Niemelä-Anttonen, Tommi Varis, Petri Vuoristo

Tampere University, Faculty of Engineering and Natural Sciences, P.O. Box 589, FI-33014, Finland

ARTICLE INFO

Keywords:
Flame spraying
Ice adhesion
Icephobic coating
Polymer coating
Lubricated coating
Icing durability

ABSTRACT

Evaluating the performance of icephobic coatings interests various industries, such as aviation, maritime, energy, and transportation. Recent developments on icephobic coatings have consistently highlighted the need for durable icephobic surfaces in cold conditions. This study investigates the icing performance and durability of lubricated polymer coatings under cyclic icing/deicing tests. Coatings were made of polyethylene and a solid lubricant and manufactured using flame spray technology. Icing was performed by accreting ice in an icing wind tunnel. Deicing was conducted by removing ice with a centrifugal ice adhesion tester. Surface properties, such as surface morphology, roughness, wettability and chemical composition, were measured before and after the cyclic tests. The results showed stable icephobic behaviour for some coatings, while the performance of others decreased over the cycles. The cyclic tests caused mechanical damage to the surfaces, producing erosion, scratches and, for some coatings, surface cracks. These defects resulted in increased surface roughness and reduced hydrophobicity. However, no chemical changes were revealed for any of the surfaces. Moreover, the causes of cracks were attributed to the difference in thermal expansion behaviour of substrate and coating materials. This result highlights the importance of materials and process parameters selection in flame sprayed coatings designed for cold applications.

1. Introduction

Ice accretion and its accumulation on surfaces represent a significant problem for several industrial applications in cold regions. Ice can compromise the working operations of several applications and, in some cases, endanger human life [1]. For instance, aviation, maritime and ground transportation, renewable energy, and offshore platforms are affected by ice formation [2], leading to economic losses and catastrophic accidents. Due to the significant influence of icing in daily operations, the past decades have seen an increased interest in developing surface solutions to minimise icing problems [3–6]. Traditionally, active ice removal methods using various forms of energy (thermal, mechanical, or pneumatic) and chemicals have represented one strategy to ensure continuous and safe working operations [7]. However, active methods are time and energy-consuming, and their sustainability issues encourage developing alternative solutions. For this reason, passive methods, which passively repel ice or retard ice formation, have emerged as potential solutions for icing problems. Passive methods mainly consist of surface treatments or protective coatings, widely referred to as icephobic coatings [8,9]. Icephobic surfaces are expected to effectively reduce ice adhesion and spontaneously promote ice shedding from exposed surfaces.

Passive icephobic methods have been classified into three main surface designs, namely superhydrophobic surfaces (SHSs), slippery liquid-infused porous surfaces (SLIPSs) and smooth surfaces made of low surface free energy materials, commonly polymers [7]. Inspired by the surface microstructure of lotus leaves [10], SHSs have been fabricated using a large variety of technologies, combining several materials and surface modification treatments [11–14]. SHSs are characterised by a micro/nano hierarchical structure with high water repellency (water contact angle >150° and water sliding angle <10°) [15]. Many researchers have hypothesised that their water repellency property would benefit surface icephobicity [16–18]. However, it was found that the long-lasting icephobic performance of superhydrophobic surfaces is limited. Several studies have shown a loss of icephobicity of SHSs, especially in environments with high humidity and sub-zero conditions

* Corresponding author at: Tampere University, Korkeakoulunkatu 6, P.O. Box 589, FI-33014 Tampere, Finland.
E-mail address: valentina.donadei@tuni.fi (V. Donadei).

https://doi.org/10.1016/j.porgcoat.2021.106614
Received 10 July 2021; Received in revised form 8 November 2021; Accepted 10 November 2021
Available online 19 November 2021

[19,20]. Moreover, mechanical damage of their hierarchical structure under consecutive icing/deicing cycles has been reported as another limitation of this surface design [13,21]. Another surface design widely tested for icephobic applications is represented by SLIPSs [7]. Inspired by the surface structure of Nepenthes pitcher plants [22], SLIPSs are characterised by a micro/nanostructure infused using various lubricating fluids based on fluorinated, silicone and hydrophilic liquids [7,23–25]. The presence of the lubricant layer ensures low surface roughness and slippery properties, which renders SLIPSs attractive for anti-icing applications. However, the instability of the lubricating layer in icing conditions represents a limitation for SLIPSs. Depletion of lubricant can lead to the degradation of icephobic properties and consequent environmental pollution [7,24,26,27]. Therefore, alternative surface designs with enhanced mechanical stability and icing durability are under consideration. An alternative surface design consists of smooth solid surfaces made of low surface free energy polymers [7]. Several polymers have been tested as potential anti-icing materials to produce smooth solid surfaces [28–33]. However, the mechanical weakness of polymeric materials may represent one challenge for this surface design [7]. Different strategies have been recently proposed to enhance the durability of polymer coatings, such as self-healing material solutions [34] or incorporation of various fillers [35]. Although smooth polymer surfaces can have less remarkable icephobic behaviour than SHSs and SLIPSs [36], their use in icephobic applications presents several advantages. In particular, polymeric coatings are cheaper and easier to prepare [36]. Moreover, they are expected to have enhanced durability over repeated icing/deicing cycles because of their more robust surface structure than the designs mentioned above [36]. Considering these advantages, the development of polymeric surfaces and assessment of their icing durability are strongly desirable. Furthermore, understanding the degradation mechanism of these surfaces in icing conditions is of fundamental importance to support future development aiming at improving their durability.

This study investigates the icing performance and durability of solid polymeric coatings under repeated icing/deicing cycles. Polymeric composite coatings were fabricated using a one-step coating method, termed flame spraying with hybrid feedstock injection in our previous work [37]. This versatile method was used to produce composite coatings consisting of two solid polymeric components: low-density polyethylene and fully hydrogenated cottonseed oil. The latter consists of a solid hydrophobic wax [38]. These coatings were named lubricated icephobic coatings (LICs) due to the lubricating additive in the coating structure [37]. The design was inspired by SLIPSs, aiming to enhance lubricant stability in icing environments [39]. Our previous work demonstrated the low ice adhesion behaviour of LICs in icing conditions. The behaviour indicates the potential of these coatings for low ice adhesion applications. Therefore, the present study aims at 1) Investigating the icing performance and durability of LICs under repeated icing/deicing cycles. 2) Understanding the effect of icing/deicing cycles on the coating surface properties, such as morphology, roughness, wettability and chemical composition, and establishing possible relationships. 3) Analysing the thermal and mechanical stresses involved in cyclic tests, which affect the coating durability, to better design coatings for cold applications.

2. Experimental procedure

2.1. Materials and coating fabrication

Commercially available low-density polyethylene powder (Plascoat LDPE, Plascoat Europe B.V., The Netherlands) and fully hydrogenated cottonseed oil powder (Lubritab® capsules, JRS PHARMA GmbH & Co. KG, Germany) were used as feedstock materials to produce composite coatings. LDPE represented the main component of the coatings, namely matrix material. Fully hydrogenated cottonseed oil constituted the minor component, namely lubricating additive. These coatings were named lubricated icephobic coatings (LICs) [37]. LICs were manufactured using flame spraying with hybrid feedstock injection, schematically represented in Fig. 1a. In this method, the matrix material was sprayed using an oxygen-acetylene flame spray gun (Castodyn DS 8000, Castolin Eutectic, Switzerland) with gas pressure for oxygen and acetylene of 4.2 bar and 0.7 bar, respectively. LDPE feedstock was fed using a powder feeder (Powder Feeder 1, Sulzer Metco 4MP, Oerlikon Metco, Switzerland) with compressed air as carrier gas. Simultaneously, the lubricating additive was sprayed externally from the gun using an injector. The injector was used to avoid direct interaction of the additive with flame and ensure its adequate feeding. The lubricant powder was fed with a second powder feeder (Powder Feeder 2, PT-10 Twin, Oerlikon Metco, Switzerland) with argon as carrier gas. Additional technical details are reported elsewhere [37]. Coatings were deposited on stainless steel substrates (EN 1.4301/2K (4N)), 30 mm × 60 mm × 1.5 mm in dimensions. Substrates were grit-blasted before spraying using aluminium oxide powder (grit size of Mesh 54). Fig. 1b summarises the sample designation together with employed process parameters.

For the coating production, process parameters, namely gun traverse speed and gun air pressure, were varied while gun spraying distance was kept constant at 250 mm. Gradual increase in gun traverse speed (from 500 to 900 mm/s) resulted in lower spraying time. However, the lower the spraying time, the lower the heat load transferred from the flame to the already deposited coating layer, thus resulting in rougher coating morphologies [33]. Similarly, the increased air pressure in the gun (from 0 to 4 bar) lowered the heat input from the flame to the powder during its flight, thus producing again rougher surfaces [37]. Additionally, post-heating of surfaces by flame was performed after coating deposition for a selected sample. Post-heating was carried out to obtain a smoother surface morphology [37].

2.2. Icephobicity and icing durability characterisation

The icephobic properties of lubricated coatings were studied using the icing test facilities at Tampere University [40]. An icing wind tunnel (IWiT) and a centrifugal ice adhesion tester (CAT) were used for the ice accretion process and the evaluation of ice adhesion strength, respectively. For these tests, the samples were placed in a climate-controlled room with monitored temperature and relative humidity (−10 °C ± 1 °C and 80% ± 5%). Once the samples reached the desired conditions, ice was accreted from supercooled water microdroplets on 30 mm × 30 mm coating areas in the IWiT. A mixed glaze type of ice was formed on the coating areas using laboratory-grade II+ water (Purelab Option-R 7/15, Elga, United Kingdom). After ice accretion, the iced samples rested in the cold room for approximately 16 h to ensure complete ice solidification. The ice was then detached from the sample surface using CAT, and ice adhesion was measured. Shear ice adhesion strength, τ_{ice} [kPa], is estimated according to Eq. 1, as the ratio of the centrifugal force F [N] at the moment of ice detachment, to the area of the iced surface A [m^2]:

$$\tau_{ice} = \frac{F}{A} = \frac{m_{ice} r \omega^2}{A} = \frac{m_{ice} r (\alpha t)^2}{A} \quad (1)$$

where m_{ice} [kg] is the known mass of the accreted ice on the specimen, r [m] is the radial spinning length at which the iced samples are spun. ω [rad/s] represents the rotational speed of the sample measured at the time t [s] of ice detachment, considering a constant angular acceleration α of 300 rpm/s. Once the ice adhesion was measured, the samples were stored at room temperature. Ice accretion and CAT testing were repeated four times to investigate icing performance and coating durability. During the cyclic icing/deicing tests, the samples experienced mechanical and thermal loads, from −10 °C to room temperature and vice versa. The ice adhesion strength was monitored at every cycle to record variations in icephobic behaviour. The ice adhesion strength was reported as the average and standard deviation of four parallel samples during each icing accretion event. A test reference surface (3M™ PTFE

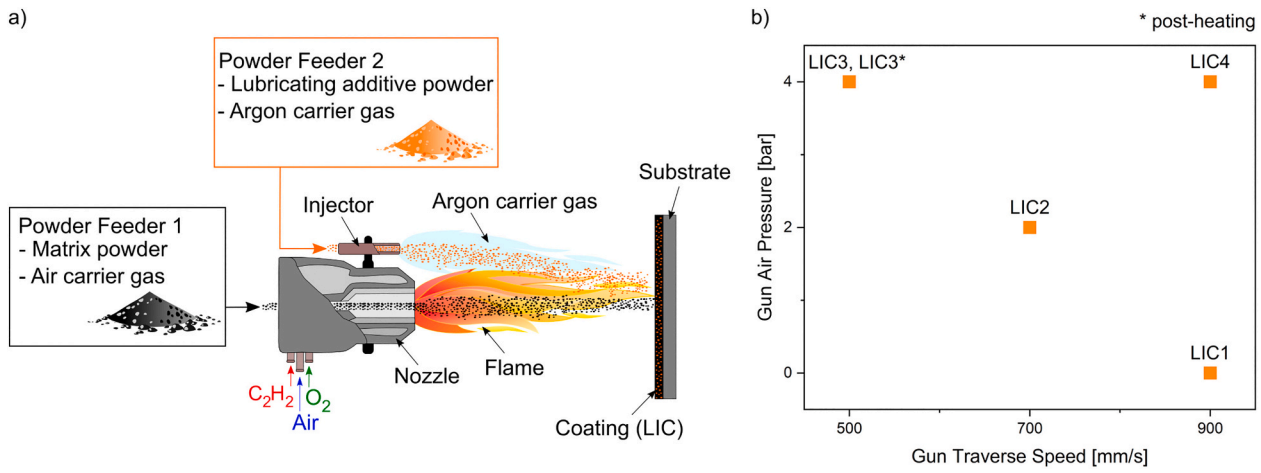

Fig. 1. Coating fabrication technique and employed process parameters. a) Schematisation of the flame spray process with hybrid feedstock injection to produce lubricated icephobic coatings (LICs), and b) summary of LIC samples studied in this work and corresponding process parameters.

Film Tape 5490, 3M, United States) was used to monitor the ice adhesion at each accretion event, considering possible variations in icing conditions [41,42].

2.3. Surface characterisation

Surface properties were investigated for as-sprayed coatings before and after the cyclic tests to analyse the effect of repeated icing/deicing. Variations in surface morphology were examined using a scanning electron microscope (SEM, Jeol, IT-500, Japan). The surface samples were cut using an automatic cut-off machine (Discotom-10, Struers ApS, Denmark). Before the analysis, the samples were dried in a desiccator and sputtered with a thin gold layer to enhance surface conductivity. An acceleration voltage of 15 keV was used to image the sample surfaces.

The surface topography was studied using an optical profilometer (contactless measuring instrument, Alicona Infinite Focus G5, Alicona Imaging GmbH, Austria). Areal roughness parameters, namely Sa, Sz and Sdr, were measured with 20× magnification objective on 2 mm × 2 mm areas at different surface locations, according to the standard ISO 25178-3 [43]. In particular, Sa represents the arithmetical mean height of the surface, Sz measures the maximum height of the surface, and Sdr signifies the developed interfacial area ratio, i.e. the percentage of additional surface area compared to an ideal plane with the size of the measurement region. Sdr value of 0% indicates a flat surface [44]. The areal roughness values were reported as the average and standard deviation of three measurements at different surface locations.

Variations in the chemical composition of surfaces were qualitatively analysed using a Fourier-transform infrared spectrometer (FTIR, Bruker Tensor 27 FT-IR spectrometer, Bruker, Sweden). The analysis was carried out using an attenuated total reflectance (ATR) sample holder (GladiATR, PIKE Technologies, United States) with a diamond crystal. Surfaces were directly placed in contact with the crystal for the analysis. The FTIR spectra were measured in the wavenumber range 4000 cm^{-1} to 600 cm^{-1} in the air at room temperature, recording 32 scans with a resolution of 4 cm^{-1}. In addition, variations in peak intensities and surface chemical composition were investigated by comparing the spectra of samples before and after the icing/deicing cycles.

Changes in wetting behaviour were analysed using a droplet shape analyser (DSA100, Krüss, Germany) in controlled conditions (22 °C ± 1 °C temperature and 60% ± 3% relative humidity). The static contact angle was measured by placing a 10 μL droplet of ultra-high purity water (MilliQ, Millipore Corporation, United States) onto the surface. The resulting apparent water contact angle was determined using the tangent method (polynomial fit of droplet shape). Tilting experiments were carried out by depositing 10 μL droplets on the surface and tilting the sample until water droplets rolled off. The roll-off angle was recorded when no droplet pinning was observed during the experiments. Both static contact angle and roll-off angle were reported as the average and standard deviation of at least five measurements on different locations of the sample surface. Moreover, the wetting behaviour in cold conditions was evaluated with a coating surface temperature of −10 °C using a temperature control chamber (Krüss TC40, Krüss, Germany). The selected temperature corresponds to our icing test temperature. The sample was placed on a Peltier stage, and the coating surface was gradually cooled from room temperature to −10 °C ± 1 °C. After the surface reached the desired temperature, the static contact angle and roll-off angle were measured. The results were reported as the average and standard deviation of at least three measurements. Further technical details on the test apparatus for sub-zero wetting experiments are described elsewhere [37].

2.4. Compositional and thermal characterisation

Thermal characterisation of coatings was carried out on as-received samples to investigate the possible effect of employed process parameters on their composition. Moreover, samples were characterised after the cyclic icing/deicing tests. Thermal analyses were performed using thermogravimetry (TG) (Netzsch TGA209F Tarsus, Netzsch, Germany) and differential scanning calorimetry (DSC) (Netzsch DSC214 Polyma, Netzsch, Germany). For TG analyses, specimens were weighted approximately 10 mg and placed in an open alumina pan. Dynamic heating was performed at 20 °C/min from 25 to 600 °C in an inert atmosphere (20 mL/min nitrogen flow). The mass change corresponding to the lubricating additive material was measured from the dynamic TG curve. For DSC analyses, specimens of approximately 10 mg were placed in a sealed concavus aluminium pans. Dynamic heating was performed from −30 °C to 150 °C at 20 °C/min in an inert atmosphere (40 mL/min nitrogen flow). The fusion enthalpies corresponding to lubricating additive and whole coating sample were measured from the dynamic curve. With this method, only the crystalline fraction of the coating is considered. The ratio between the two measured enthalpies gives a qualitative indication of the lubricating additive content in the coating. The results were reported as the average and standard deviation of at least three measurements. Additional details on the methods are described in the Supporting Information.

Coefficients of thermal expansion (CTEs) of feedstock materials, free-standing coatings, and substrate were evaluated using a dilatometer (DIL 402 Expedis® Select, Supreme, Netzsch, Germany) with a silica probe. This analysis was carried out to understand the behaviour of the coating structure (composite coating deposited on stainless steel

substrate) under repeated thermal loads experienced during icing/deicing tests. The samples were analysed from −15 °C to 35 °C with a heating rate of 1 °C/min in an inert atmosphere (50 mL/min helium flow). CTE values were reported as the average and standard deviation of at least three measurements in the range of −10 °C to 25 °C. The operating temperatures of the coatings were within this range during the icing/deicing cycles.

3. Results and discussion

3.1. Icephobic behaviour and icing durability

The tendency of a surface to repel ice is commonly defined as icephobicity [9]. However, different definitions of icephobicity have been considered in the literature. Some researchers note icephobicity as the distinctive characteristic of surfaces to weakly adhere to ice [5,45,46]. For this definition, the ice adhesion is measured using different ice adhesion tests [47,48]. The lower the measured ice adhesion, the higher the surface icephobicity. However, the employed test method, ice type, temperature, and other test variables strongly influence the obtained numerical adhesion values [42,45]. Other researchers consider icephobicity as the ability of surfaces to repel incoming cold water droplets and delay or inhibit ice nucleation [12,14,49]. For this definition, icephobicity is tested with impact droplet experiments on cold surfaces or freezing delay experiments. In this work, icephobicity was evaluated by measuring the shear ice adhesion strength of mixed glaze ice accreted in the IWiT. The ice adhesion was measured using CAT. For this specific test and ice type [24,29], ice adhesion values of 50 kPa and 100 kPa indicate the low and medium-low ice adhesion limit, respectively. Fig. 2a summarises the ice adhesion results at the first icing/deicing cycle and corresponding surface roughness values for all coatings and reference material. Fig. 2b shows the visual appearance of the ice block accreted on the coating surface at −10 °C.

At the first cycle, all lubricated coatings demonstrated low ice adhesion behaviour with values below 50 kPa. From the results, it was evident that the employed process parameters influenced the icephobic behaviour of coatings. Interestingly, the average ice adhesion value decreased with the increased gun air pressure during coating production (from LIC1 with no air to LIC3 with 4 bar air pressure), reaching the lowest value of 23 kPa ± 6 kPa for coating LIC3 (4 bar air pressure and 500 mm/s traverse speed). Moreover, if post-heating by flame was performed for LIC3, the ice adhesion increased approximately 61% (LIC3* compared to LIC3). If a faster traverse speed of the gun was employed, ice adhesion rose approximately 35% (LIC4 with 900 mm/s compared to LIC3 with 500 mm/s traverse speed). Surprisingly, ice adhesion decreased with increased surface roughness, passing from LIC1 to LIC3. Previous research demonstrated that the increased surface roughness promotes mechanical interlocking between ice and surface, thus resulting in enhanced ice adhesion [50]. Therefore, another factor could probably influence the icephobicity of these surfaces. However, this relationship was verified when an even rougher surface was produced, passing from LIC3 to LIC4, fabricated using the highest air pressure in the flame gun and traverse speed.

Coatings underwent repeated icing/deicing cycles, and changes in ice adhesion were monitored to assess the durability of LICs in icing conditions. Previous studies have reported the durability of surfaces tested under a few [24,46,51] until over 100 [5,52,53] icing/deicing cycles. In some studies, the icing procedure consists of forming ice by pouring water in a mould placed on the samples [30,54,55], while deicing comprises heating the sample until ice thaws [53,56]. Compared to methods where deicing occurs by applying shear or normal stresses to an adherent block of ice (accreted or moulded ice), these before mentioned deicing methods are significantly less severe for tested surfaces [46]. Therefore, the icing durability of surfaces should be carefully discussed when comparing different studies, considering employed icing/deicing methods, involved classes of materials and type of ice. Similarly significant, the number of performed cycles and their severity on the surface depends on employed icing test setups and icing/deicing methods. In our icing method, mixed glaze ice was accreted from accelerated supercooled microdroplets. These droplets penetrated the micro and macro-features of the surfaces, thus intimately anchoring the surface microstructure. Ice was then removed by centrifugal forces (shear stress distribution at the interface) and consecutively accreted and detached four times. Fig. 3 presents the ice adhesion values measured at each cycle.

From the first to the second cycle, an increase in ice adhesion was noticed for all coatings. This result indicated decreased surface icephobicity. Ice adhesion increase was probably due to changes in surface properties produced during the cyclic tests. Previous studies on the icing performance of polymeric coatings have reported a similar behaviour over the cycles using the CAT deicing method [46,57]. Both variations in surface chemistry and mechanical damage of surfaces have been considered the leading causes of reduced icephobic performances due to consecutive ice removal [21,46,51,56,58,59]. After the second cycle, a further increase in ice adhesion was observed for all coatings, except for LIC1, which showed a more stable icephobic behaviour. Similarly,

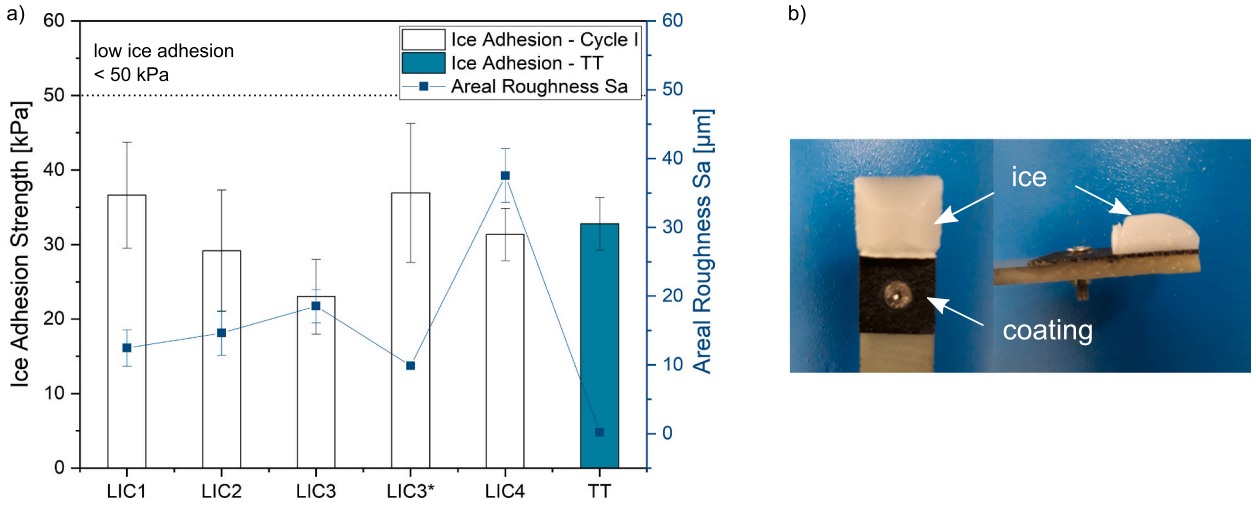

Fig. 2. Icephobic behaviour of lubricated icephobic coatings measured at −10 °C with mixed glaze ice. a) Ice adhesion strength and related surface roughness Sa values of LICs and Teflon tape (TT), which represents the reference material for the ice adhesion test, and b) accreted mixed glaze ice (white block) on a lubricated icephobic coating sample.

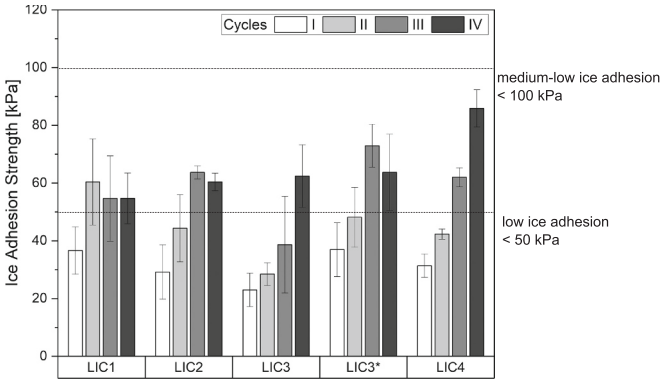

Fig. 3. Ice adhesion results for all LICs over four icing/deicing cycles.

coatings LIC2 and LIC3* seemed to stabilise their icephobicity after the third cycle. Conversely, coatings LIC3 and LIC4 showed gradual degradation until the fourth cycle. Due to the relevant variation in icephobic behaviour, four cycles were considered sufficient to evaluate the icing performance in this study. Despite degraded icephobic character over the cycles, all LICs maintained ice adhesion strength below the limit of 100 kPa, thus retaining their icephobicity within the medium-low ice adhesion level.

Differences in surface properties of LICs might have produced variations in ice adhesion values over the cycles. For example, LIC1 was characterised by a relatively smooth surface morphology compared to other coatings, as shown by the roughness values in Fig. 2a. Smooth surfaces reduce the possibility of mechanical interlocking of ice [50]. This property can be beneficial during repeated icing/deicing, resulting in lower surface damage by ice [60]. Moreover, coating composition could play a role in determining the icephobic behaviour over the cycles. The compositional analysis of LICs via thermal characterisation demonstrated a lower amount of lubricating additive for the coating LIC1 compared to all other coatings, as shown in supporting Fig. S3. This result was justified by the higher heat input employed in the processing of this coating (no additional air in the flame gun), which could reduce the deposition efficiency of the lubricating additive [37]. Furthermore, the lower amount of lubricating additive in the coating structure could increase the mechanical resistance of the coating to ice shedding during deicing. Therefore, the combination of both surface topography and content of lubricating additive could have determined the more stable icephobicity of LIC1. This result provides relevant information for further research in the design of LICs, aiming at enhancing icing performance and durability.

3.2. *Effect of icing/deicing cycles on topography and coating morphology*

Fig. 4 represents the surface topography and micrographs of all coatings before and after four icing/deicing cycles. Topographical representations of surfaces evidenced different morphologies depending on the employed process parameters. In general, for flame sprayed polymer coatings, the higher the heat input during the process, the higher the degree of melting of the feedstock powders and the lower the obtained surface roughness. In particular, unmelted particles were evident on LIC3 and LIC4 surfaces when low heat input of the flame (gun air pressure of 4 bar) was employed during spraying. The unmelted particles corresponded to the polyethylene matrix material, considering the lubricating additive completely melted with these specific process conditions [37]. Moreover, the micrographs visibly showed differences in coating surface morphologies before and after cyclic icing/deicing tests.

All coatings were mechanically damaged during the cyclic tests, which caused the wearing of polymeric surfaces. Micrographic analyses revealed different defects, such as surface erosion, surface scratches and cracks, as shown in Fig. 5. Surface defects, most commonly scratches, were produced for all coatings, and these were also visible from optical analyses, as shown in supporting Fig. S4. A few scratches were already evident before icing from the micrographs of LIC1 and LIC2, as shown in Fig. 4. These were also noticed in supporting Fig. S4. Therefore, a few scratches could have been formed during sample handling before the cycles and sample preparation procedure, considering the softness of the polymeric components and, particularly, of the lubricating additive. Moreover, cracking of the surfaces was detected between the unmelted particles for samples LIC3 and LIC4. The causes of cracking will be analysed and discussed in Section 3.4. However, cracking could be avoided for other coatings when lower air pressure was added to the flame gun (no air for LIC1 and 2 bar for LIC2), and post-heating was performed after coating deposition (LIC3*). From the results, mechanical damage of surfaces could represent one cause of the gradual increase in ice adhesion strength for LICs over the cycles (Fig. 3), according to previous studies [35,46,58,60].

Fig. 6 represents the variations in areal roughness parameters (Sa, Sz, Sdr) before and after the icing/deicing cycles. Fig. 6a reports variations in Sa and Sz parameters, and Fig. 6b the Sdr values. Supporting Table S1 collects the experimental data. From the results, the employed process parameters influenced the initial surface roughness of LICs. The lower the heat input of the flame gun, the rougher the surfaces (from LIC1 with no additional air to LIC3 and LIC4 with 4 bar). The lower heat input caused partial melting of the polymer particles, resulting in coatings with higher surface roughness and developed interfacial areas (LIC3 and LIC4 compared to other coatings). Post-heat treatment by flame produced remelting of polymers, reducing the coating surface roughness (LIC3* compared to LIC3). After the cycles, a slight increase in average height, Sa, and maximum height, Sz, was verified for all coatings. However, in most cases, the Sa and Sz values varied within the standard deviation. This slight rise can be justified by the produced mechanical damage, which increased the surface roughness [35]. A more significant difference was measured for the developed interfacial area value, Sdr. The increased area could promote mechanical interlocking between ice and surface features, thus probably justifying the increased ice adhesion strength over the cycles [50]. However, a relationship between the degree of increased interfacial area and the increased ice adhesion could not be systematically established in this study for LICs. Possibly, additional factors could influence icephobicity, and, therefore, further investigations are needed to establish correlations.

3.3. *Effect of icing/deicing cycles on wettability and surface chemistry*

Wettability of surfaces is commonly considered one of the critical properties to predict the icephobic behaviour of surfaces [30,31]. Moreover, wetting properties have helped to understand the variations in icing performance and durability of coatings under repeated icing/deicing cycles [36,46,57,61,62]. Fig. 7 shows the results of the wetting experiments before and after four icing/deicing cycles. Fig. 7a compares the apparent water contact angle (WCA) values obtained for room temperature experiments and Fig. 7b for cold temperature conditions. The latter was carried out to understand better the wetting behaviour of surfaces in conditions as similar as possible to the icing test environment [63,64].

From the wetting results before the cycles, LICs demonstrated different wetting behaviour. The different behaviour was more evident for the room temperature experiments than for the cold experiments. For room temperature experiments, the smoothest surfaces of this study, namely LIC1 and LIC3*, showed apparent water contact angles higher than 120°. It is well known that water contact angles never exceed 120° in a Wenzel wetting state for the most hydrophobic solids [65,66]. Therefore, these results suggested that the surfaces were partially wetted, and air pockets were probably trapped beneath the water droplets [67]. The wetting behaviour was better explained by the micrographs of surface morphologies presented in Fig. 8.

The micrographs showed that LIC1 and LIC3* were characterised by

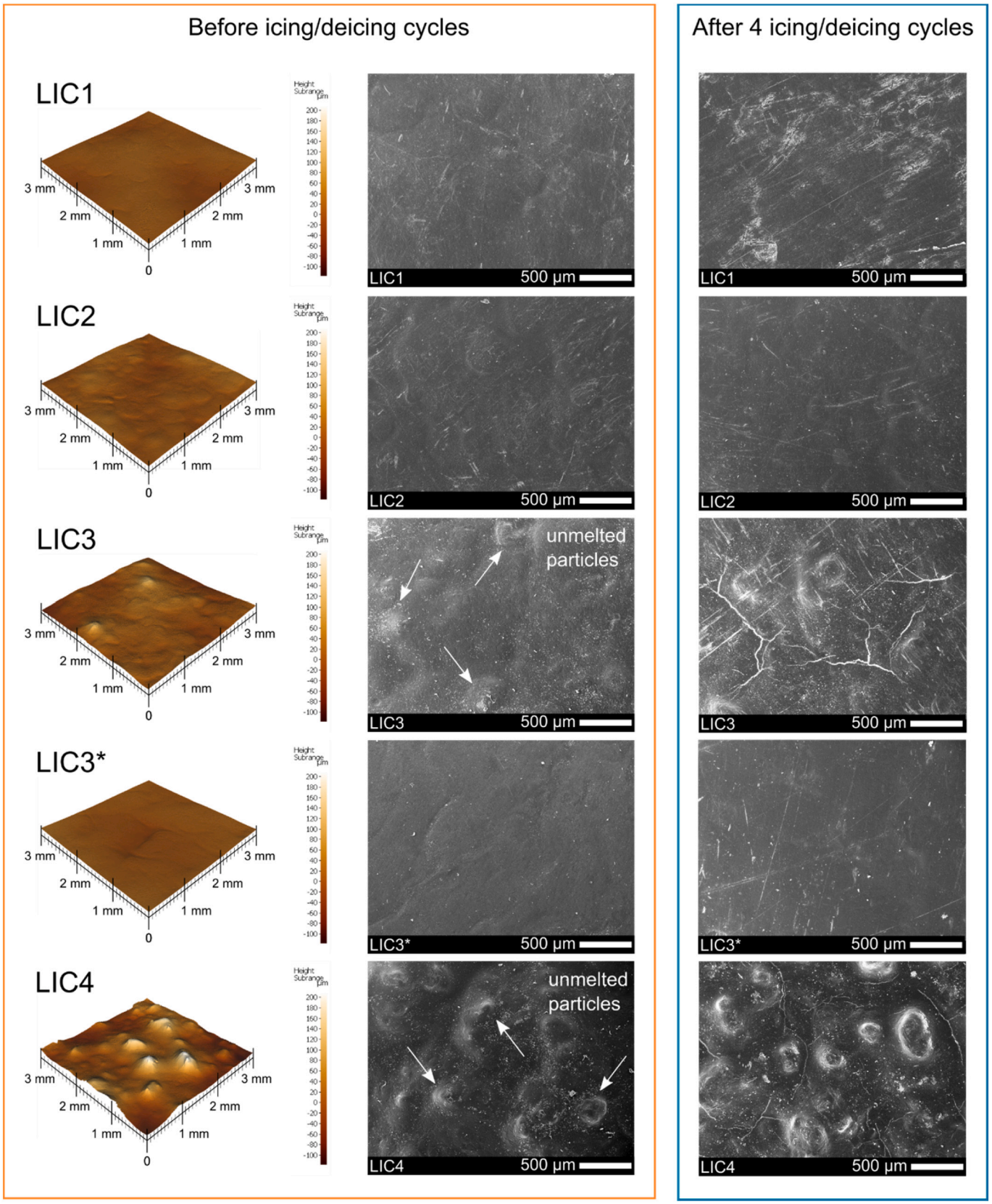

Fig. 4. Surface topographies and morphologies of the coatings before and after four icing/deicing cycles. Optical profilometer images of the surface areas before icing/deicing cycles (left). The colour scale in the images indicates the height of the surface: lighter colour for peaks and a darker colour for valleys. Electron microscope images of the coating surface before (middle) and after four icing/deicing cycles (right).

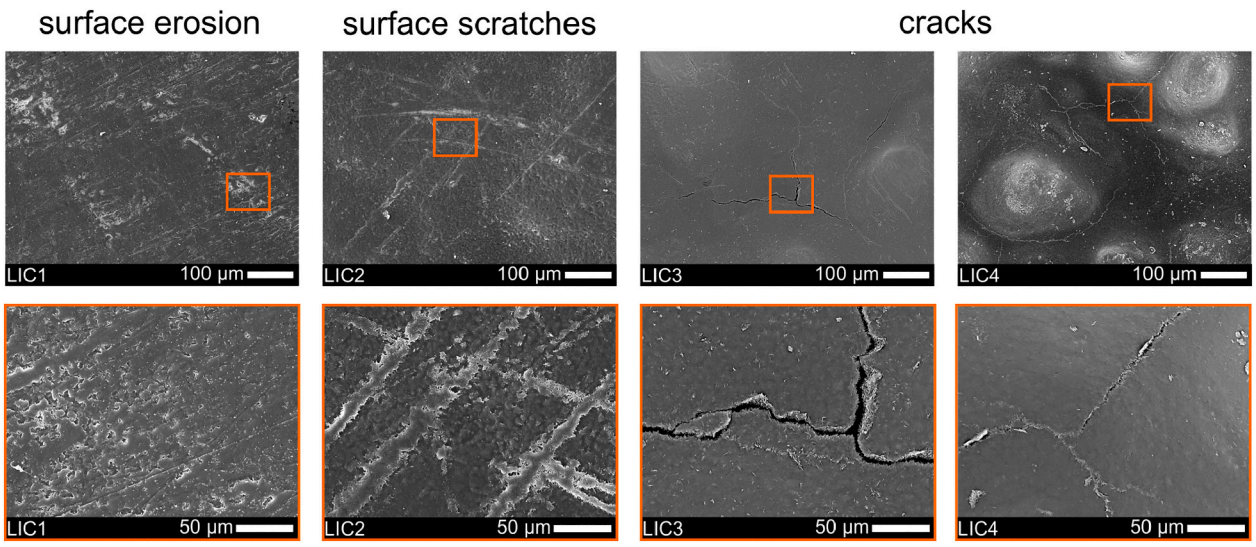

Fig. 5. Surface defects (indicated by orange squares) of LICs after four icing/deicing cycles at different magnifications. From left to right, the micrographs show surface erosion, surface scratches, and cracks.

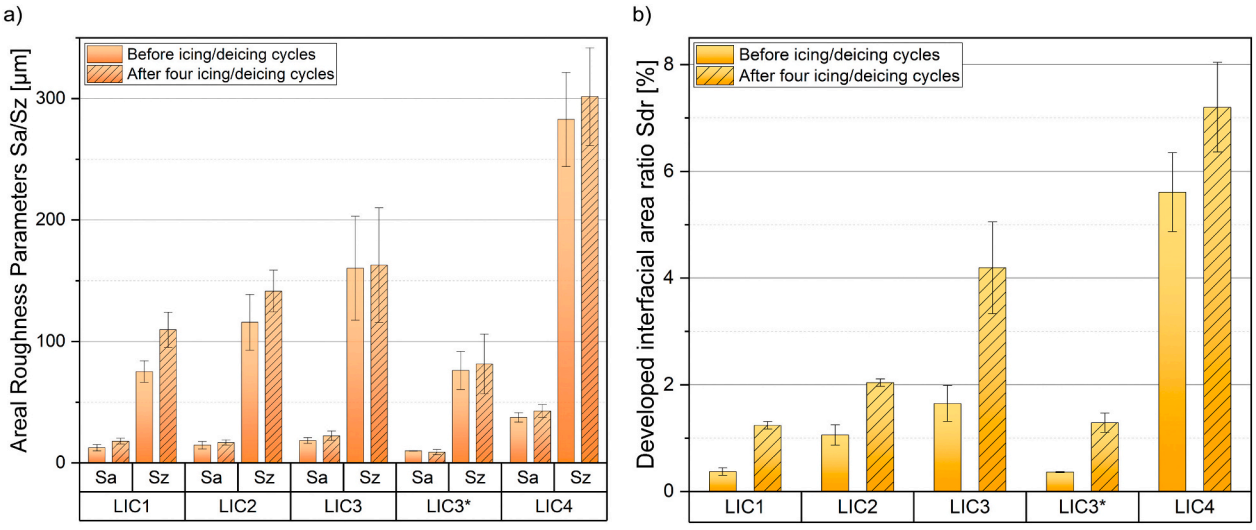

Fig. 6. Areal roughness parameters of LICs before and after four icing/deicing cycles. a) Areal roughness parameters (Sa and Sz), and b) developed interfacial area ratio (Sdr). No patterned columns and patterned columns indicate the parameters before and after four icing/deicing cycles.

finer surface features compared to all other coatings. These features were similar to small protuberances and resulted from the process parameters selected during coating production. Surface protuberances probably promoted the presence of air pockets trapped underneath water droplets in the wetting experiments. This resulted in a mixed Cassie-Wenzel wetting state with droplets showing contact angles higher than 120°. Moreover, the presence of air pockets was evidenced by the wetting results at cold temperature. A significant decrease in water contact angles was noticed in these conditions for LIC1 and LIC3* compared to room temperature experiments. Cold surfaces induce water condensation from the droplets to the surface microstructure. Condensation phenomena eliminate the trapped air pockets, thus reducing the measured water contact angle [63,68]. For more details on the wetting state of these coatings, the authors refer to their previous study [37]. From the results at room temperature, the surfaces retained their hydrophobic character after four icing/deicing cycles (apparent WCA > 90° for all coatings). A slight decrease of apparent WCA was revealed for all coatings, except for the rougher surface of this study (LIC4). However, in most cases, the values fall within the standard deviation of the measurements. Conversely, the decrease of WCA was more evident in the experiments performed in cold conditions. In these experiments, the water condensates onto the surface features, thus reducing the presence of possible air pockets beneath the drops [69]. This phenomenon results in decreased apparent WCA when passing from a mixed Cassie-Wenzel wetting state (room temperature experiments) to a Wenzel wetting state (cold temperature experiments) using the same volume of water droplets [37,65]. Moreover, roll-off angles were measured, but no droplet mobility was detected (water roll-off angle >90° for all surfaces). Considering the icephobic performance of LICs over the cycles, the wetting results supported the work of other studies linking the decrease of icephobicity with the decrease of surface hydrophobicity after icing/deicing cycles [13,46,57,58,61].

The decrease in surface hydrophobicity can depend on variations in surface roughness and chemistry [65]. In this study, variations in surface roughness were produced by mechanical damage during the cyclic tests. Moreover, mechanical damage could generate local modifications of surface chemistry due to possible material removal. In addition, the interaction of polymers with water, ice and humid environment can

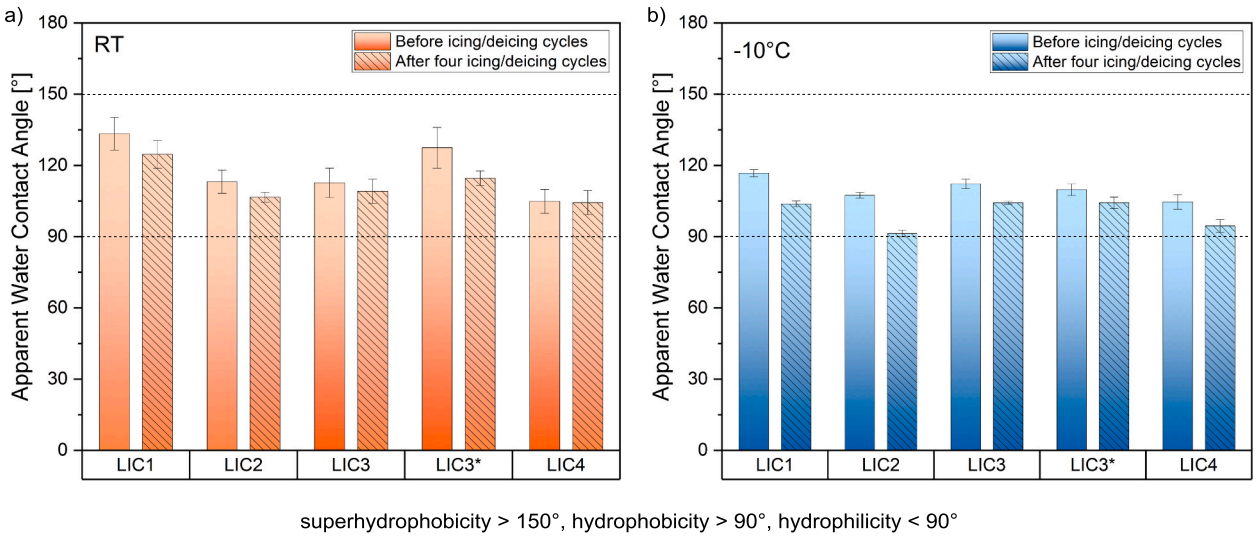

Fig. 7. Results of the wetting experiments before and after four icing/deicing cycles. Apparent WCA at a) room temperature, and b) −10 °C surface temperature, which corresponds to the icing test temperature.

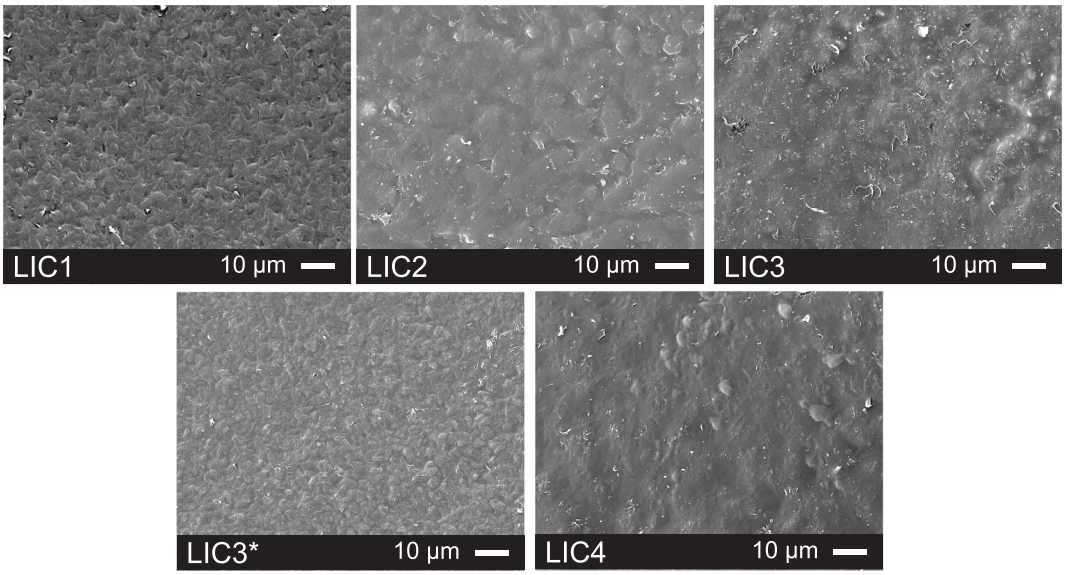

Fig. 8. Micrographs of the surface morphologies for all as-sprayed lubricated icephobic coatings.

cause chemical changes due to hydrolysis [70]. From the chemical analyses before and after the cycles, no variations in surface chemistry were revealed, as shown in the FTIR spectra of supporting Fig. S5. Therefore, the cause of the decreased hydrophobicity of surfaces was primarily related to mechanical damage. The soft additive, which has higher hydrophobicity than the matrix material [37], could have been locally removed from the surface during deicing. This local removal might contribute to the slight decrease in surface hydrophobicity. In conclusion, the results suggested that the decrement in icephobicity over the cycles was mainly due to mechanical damage, which produced variations of surface properties.

3.4. *Effect of icing/deicing cycles on coating cracking behaviour*

Surface cracking represents one of the possible mechanical failures of coatings [70] and can occur due to several factors. For example, cracks can form due to impact with objects, abrasion, degradation by ultraviolet irradiation, hydrolysis, contaminants on the substrate, and internal and external stresses [70]. In this study, micrographs in Fig. 4 and Fig. 5 revealed surface cracks between the unmelted matrix particles for coatings LIC3 and LIC4 after icing/deicing cycles. Presumably, the unmelted particles visible on the surfaces were surrounded by lubricant-rich regions.

During repeated icing/deicing tests, coatings experienced cyclic thermal and mechanical stresses, as schematically described at each test stage in Fig. 9. At the first stage, coatings (LICs on a stainless steel substrate) were cooled from room temperature to the icing test conditions (from 22 °C ± 3 °C and relative humidity of 20% ± 5% to −10 °C ± 1 °C and relative humidity of 80% ± 5%). During cooling, the coating and the substrate shrink depending on their coefficient of thermal expansion (CTE). If the coating has higher CTE than the substrate, the latter can constrain the coating from shrinking, thus inducing tensile stresses to the coating [70,71]. CTEs of 15.1 ± 0.1 × 10^{-6} °C^{-1} and 182.4 ± 1.7 × 10^{-6} °C^{-1} were measured for the stainless steel substrate and free-standing LIC3 coating, respectively. The experimental CTE data is reported in supporting Fig. S6 and Table S2. The results indicated a

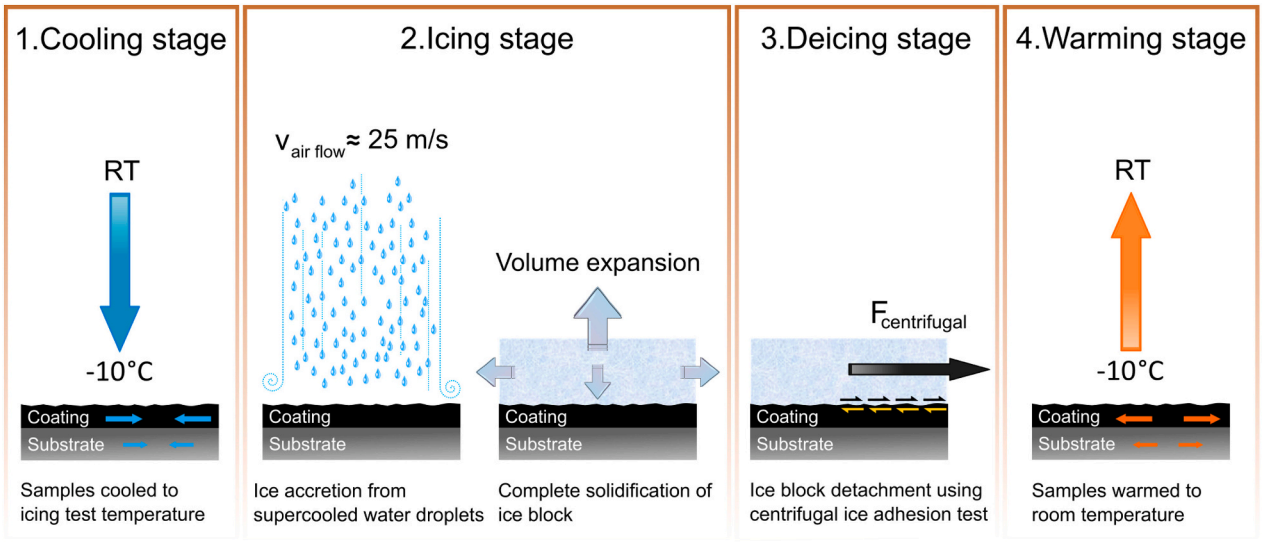

Fig. 9. Stages of the cyclic icing/deicing tests. 1) Cooling stage of the samples from room temperature to the icing test temperature. 2) Icing stage with the accretion of mixed glaze ice from supercooled water droplet in the icing wind tunnel and solidification of the ice block. 3) Deicing stage with the removal of the ice block using the centrifugal ice adhesion tester. 4) Warming stage with samples stored at room temperature.

significant mismatch between the CTEs. If induced tensile stresses exceed the fracture resistance of the coating, cracking can occur [72,73], especially considering the lower mechanical properties of the lubricant-rich regions. At the second stage, a cold wind flow accelerated the supercooled water microdroplets towards the coating surfaces placed in the icing wind tunnel. No stresses caused by water droplets impact on surfaces (possible peening stresses transferred to the coating surface due to impact) were considered in this analysis. A block of mixed glaze ice was then accreted from the continuous impact of supercooled micro-droplets. Immediately after accretion, the mixed glaze ice block comprised both fractions of liquid and solidified water. The block was rested to allow complete solidification, causing the liquid water to expand. Water expansion can cause some damage to the coating surface due to significant developed interfacial stresses [60]. At the third stage, a gradual centrifugal force was applied to the iced sample until ice detachment occurred, forming mechanical stresses (normal and shear stresses) at the ice-coating interface [40]. At the fourth stage, the samples were warmed to room temperature. The materials expanded and dried in this environment, and again mismatch of CTEs can induce stresses. The cycles were then repeated from the first stage.

To study more in detail the effect of the substrate material on cracking behaviour, LIC3 coating was sprayed on an LDPE substrate,

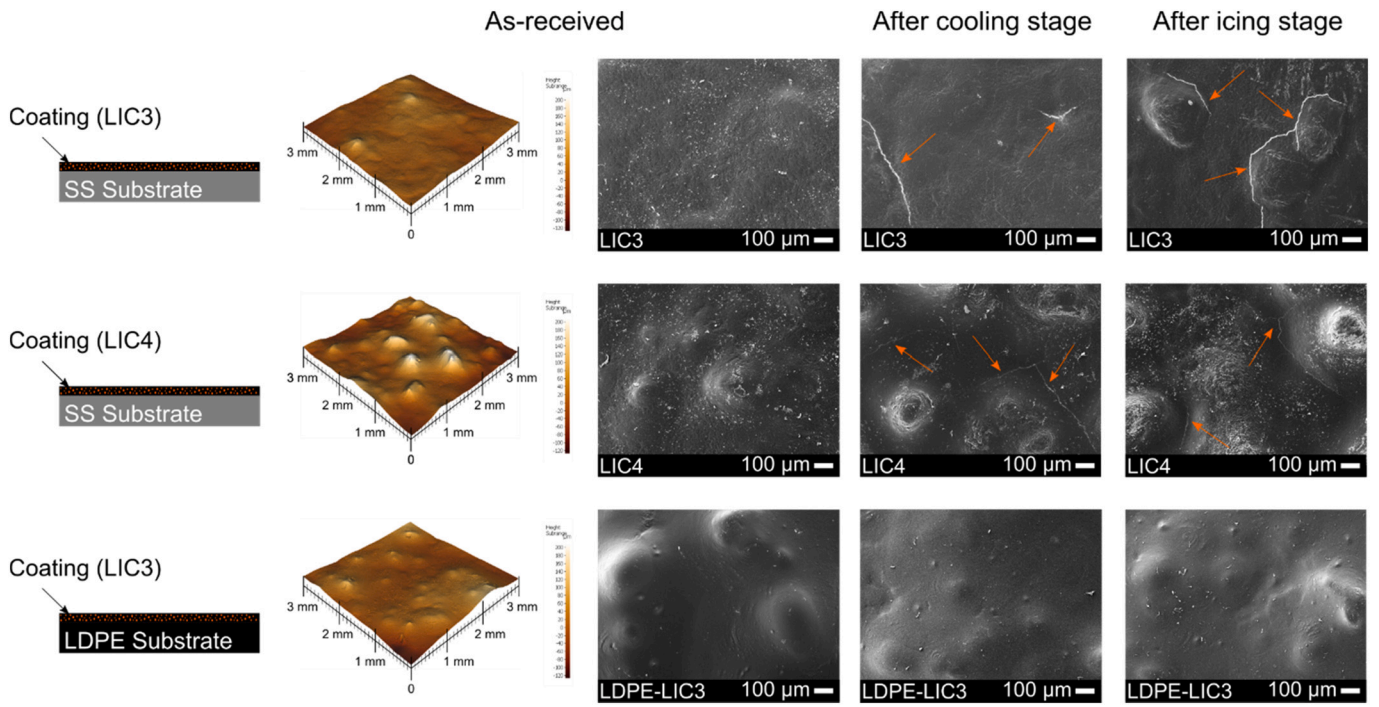

Fig. 10. Influence of the material substrate on the cracking behaviour of LICs. The schematisation of coating samples and related surface topographical images (left). Surface micrographs of the coatings at different stages of the icing/deicing cycles, such as as-received, after cooling stage, after icing/deicing stage (middle and right). Orange arrows indicate cracks.

which was prepared from the same grade as the matrix material of LICs. The CTE of the LDPE substrate was $188.3 \pm 1.4 \times 10^{-6}\ ^{\circ}C^{-1}$ and thus similar to the CTE of the coating. Icing/deicing cycles were performed as for the coatings sprayed on stainless steel substrate, and the surface morphologies were compared at every stage of the test. Fig. 10 shows the schematisation of the coating structures, their topography and surface morphology at different stages of the icing/deicing cycles.

It was noticed that cracking occurred already after the cooling stage of the icing/deicing tests for coatings sprayed on stainless steel substrates. This result indicated that cracking in the lubricant-rich regions was mainly induced by thermal stresses. The lubricant-rich regions presumably have lower mechanical properties than the matrix material. Therefore, these weaker regions of the coatings were probably more prone to cracking than others. However, cracking behaviour was prevented when the coating was sprayed on the LDPE substrate, which had thermal expansion properties similar to the coating material. Consequently, causes of cracking behaviour were considered to be directly related to the CTE mismatch and cohesive strength of the coating.

In addition, other hypotheses on the causes of cracking were considered. For example, residual tensile stresses could be present in the coating after its fabrication and solidification, thus further contributing to cracking [71]. Therefore, an annealing treatment was performed to relax possible residual stresses before cyclic icing/deicing tests. However, the coatings showed no change in cracking behaviour after annealing, as revealed in supporting Fig. S7, and the heat treatment was no beneficial to avoid crack formation. Another hypothesis on the causes of cracking was related to possible water absorption during the cyclic tests. Water absorption could then produce swelling of polymers and shrinking when drying occurs, thus inducing coating cracking [70]. However, this was not relevant in our study since cracking occurred during the first cooling stage for samples isolated (stored in sealed plastic containers) from possible contact with water, ice and humid environment. Furthermore, other coating properties could influence the formation of cracks, such as coating thickness, polymer properties in sub-zero conditions, Poissons's ratio and other variables [70,73]. Therefore, further studies, which consider these variables, should be considered. In conclusion, investigating possible causes of cracking was relevant for the design of flame-sprayed coatings for cold applications, thus highlighting the importance of selected materials (coating and substrate combination) and/or process parameters.

4. Conclusions

The study investigated the icing behaviour of flame sprayed lubricated icephobic coatings (LICs) and their durability under repeated icing/deicing cycles. LICs consisted of a matrix material made of low-density polyethylene and a lubricating additive made of solid fully hydrogenated cottonseed oil. Coatings were fabricated using flame spraying with hybrid feedstock injection. It was found that LICs exhibited low ice adhesion values at the first icing/deicing cycle. Over repeated cycles, some coatings (LIC1, LIC2, LIC3*) tended to stabilise their icephobic behaviour. In particular, LIC1 showed the most stable icephobic behaviour. This coating was characterised by a reduced amount of lubricating additive in its structure and relatively smooth morphology. Conversely, rougher coatings (LIC3, LIC4) showed a gradual decrease in their icephobicity over the cycles. However, all coatings retained their icephobicity after the cycles, residing below the low-medium ice adhesion limit of 100 kPa for this ice adhesion test. Repeated cycles caused mechanical damage to surfaces. This damage produced increased surface roughness and decreased hydrophobic character of the coatings. In addition, surface cracks were revealed in some coatings (LIC3, LIC4) after icing/deicing cycles. The causes of cracking behaviour were correlated to the significant difference in coefficients of thermal expansion between the coatings and the substrate material. It was demonstrated that cracking behaviour could be avoided using a substrate material with thermal expansion properties more similar to the coatings. These findings have significant implications in the development of coatings for cold applications, thus highlighting the importance of material combination and process parameters selection. Future studies will aim at further enhancing the durability of LICs in icing conditions. Moreover, their performance will be investigated under different environmental stresses.

CRediT authorship contribution statement

Valentina Donadei: Conceptualization, Methodology, Investigation, Visualization, Writing – original draft. **Heli Koivuluoto:** Conceptualization, Supervision, Funding acquisition, Resources, Writing – review & editing. **Essi Sarlin:** Supervision, Writing – review & editing. **Henna Niemelä-Anttonen:** Methodology, Writing – review & editing. **Tommi Varis:** Writing – review & editing. **Petri Vuoristo:** Supervision, Funding acquisition, Resources, Writing – review & editing.

Declaration of competing interest

The authors declare that they have no known competing financial interests or personal relationships that could have appeared to influence the work reported in this paper.

Acknowledgements

Authors thank the LubISS (Lubricant Impregnated Slippery Surfaces) project that received funding from the European Union's Horizon 2020 research and innovation programme under the Marie Sklodowska-Curie Grant Agreement No. 722497. V.D. acknowledges the Faculty of Engineering and Natural Sciences of Tampere University for the financial support. In addition, Mr. Anssi Metsähonkala and Mr. Jarkko Lehti from Tampere University are acknowledged for technical support in the flame spray process. M.Sc. Enni Hartikainen and Mr. Jarmo Laakso from Tampere University are thanked for assisting in icing testing and dilatometer experiments, respectively. This work made use of Tampere Microscopy Center facilities at Tampere University.

Appendix A. Supplementary data

Supplementary data to this article can be found online at https://doi.org/10.1016/j.porgcoat.2021.106614.

References

[1] M. Farzaneh, Atmospheric Icing of Power Networks, Springer Netherlands, Dordrecht, 2008, https://doi.org/10.1007/978-1-4020-8531-4.
[2] M. Grizen, M.K. Tiwari, Icephobic surfaces: features and challenges, in: K.L. Mittal, C.-H. Choi (Eds.), Ice Adhes. Mech. Meas. Mitig, Wiley, 2020, pp. 417–466, https://doi.org/10.1002/9781119640523.ch14.
[3] P. Irajizad, S. Nazifi, H. Ghasemi, Icephobic surfaces: definition and figures of merit, Adv. Colloid Interf. Sci. 269 (2019) 203–218, https://doi.org/10.1016/j.cis.2019.04.005.
[4] R. Menini, M. Farzaneh, Advanced icephobic coatings, J. Adhes. Sci. Technol. 25 (2011) 971–992, https://doi.org/10.1163/016942410X533372.
[5] K. Golovin, S.P.R. Kobaku, D.H. Lee, E.T. DiLoreto, J.M. Mabry, A. Tuteja, Designing durable icephobic surfaces, Sci. Adv. 2 (2016), e1501496, https://doi.org/10.1126/sciadv.1501496.
[6] T.M. Schutzius, S. Jung, T. Maitra, P. Eberle, C. Antonini, C. Stamatopoulos, D. Poulikakos, Physics of icing and rational design of surfaces with extraordinary icephobicity, Langmuir 31 (2015) 4807–4821, https://doi.org/10.1021/la502586a.
[7] S. Ozbay, H.Y. Erbil, On the relationship between surface free energy and ice adhesion of flat anti-icing surfaces, in: Ice Adhes, Wiley, 2020, pp. 187–215, https://doi.org/10.1002/9781119640523.ch7.
[8] M.J. Kreder, J. Alvarenga, P. Kim, J. Aizenberg, Design of anti-icing surfaces: smooth, textured or slippery? Nat. Rev. Mater. 1 (2016), 15003 https://doi.org/10.1038/natrevmats.2015.3.
[9] H. Sojoudi, M. Wang, N.D. Boscher, G.H. McKinley, K.K. Gleason, Durable and scalable icephobic surfaces: similarities and distinctions from superhydrophobic surfaces, Soft Matter 12 (2016) 1938–1963. https://doi.org/10.1039/C5SM02295A.

[10] C. Neinhuis, W. Barthlott, Characterization and distribution of water-repellent, self-cleaning plant surfaces, Ann. Bot. 79 (1997) 667–677, https://doi.org/10.1006/anbo.1997.0400.
[11] Y. Lin, H. Chen, G. Wang, A. Liu, Recent progress in preparation and anti-icing applications of superhydrophobic coatings, Coatings 8 (2018) 208, https://doi.org/10.3390/coatings8060208.
[12] L. Wang, Q. Gong, S. Zhan, L. Jiang, Y. Zheng, Robust anti-icing performance of a flexible superhydrophobic surface, Adv. Mater. 28 (2016) 7729–7735, https://doi.org/10.1002/adma.201602480.
[13] S. Farhadi, M. Farzaneh, S.A. Kulinich, Anti-icing performance of superhydrophobic surfaces, Appl. Surf. Sci. 257 (2011) 6264–6269, https://doi.org/10.1016/j.apsusc.2011.02.057.
[14] L. Cao, A.K. Jones, V.K. Sikka, J. Wu, D. Gao, Anti-icing superhydrophobic coatings, Langmuir 25 (2009) 12444–12448, https://doi.org/10.1021/la902882b.
[15] A. Nakajima, K. Hashimoto, T. Watanabe, Recent studies on super-hydrophobic films, in: Mol. Mater. Funct. Polym, Springer Vienna, Vienna, 2001, pp. 31–41, https://doi.org/10.1007/978-3-7091-6276-7_3.
[16] S. Zhang, J. Huang, Y. Cheng, H. Yang, Z. Chen, Y. Lai, Bioinspired Surfaces with superwettability for anti-icing and ice-phobic application: concept, mechanism, and design, Small 13 (2017), 1701867, https://doi.org/10.1002/smll.201701867.
[17] Q. Li, Z. Guo, Fundamentals of icing and common strategies for designing biomimetic anti-icing surfaces, J. Mater. Chem. A 6 (2018) 13549–13581, https://doi.org/10.1039/c8ta03259a.
[18] J. Lv, Y. Song, L. Jiang, J. Wang, Bio-inspired strategies for anti-icing, ACS Nano 8 (2014) 3152–3169, https://doi.org/10.1021/nn406522n.
[19] S. Jung, M. Dorrestijn, D. Raps, A. Das, C.M. Megaridis, D. Poulikakos, Are superhydrophobic surfaces best for icephobicity? Langmuir 27 (2011) 3059–3066, https://doi.org/10.1021/la104762g.
[20] L. Oberli, D. Caruso, C. Hall, M. Fabretto, P.J. Murphy, D. Evans, Condensation and freezing of droplets on superhydrophobic surfaces, Adv. Colloid Interf. Sci. 210 (2014) 47–57, https://doi.org/10.1016/j.cis.2013.10.018.
[21] S.A. Kulinich, S. Farhadi, K. Nose, X.W. Du, Superhydrophobic surfaces: are they really ice-repellent? Langmuir 27 (2011) 25–29, https://doi.org/10.1021/la104277q.
[22] T.S. Wong, S.H. Kang, S.K.Y. Tang, E.J. Smythe, B.D. Hatton, A. Grinthal, J. Aizenberg, Bioinspired self-repairing slippery surfaces with pressure-stable omniphobicity, Nature 477 (2011) 443–447, https://doi.org/10.1038/nature10447.
[23] M. Zhang, J. Yu, R. Chen, Q. Liu, J. Liu, D. Song, P. Liu, L. Gao, J. Wang, Highly transparent and robust slippery lubricant-infused porous surfaces with anti-icing and anti-fouling performances, J. Alloys Compd. 803 (2019) 51–60, https://doi.org/10.1016/j.jallcom.2019.06.241.
[24] H. Niemelä-Anttonen, H. Koivuluoto, M. Tuominen, H. Teisala, P. Juuti, J. Haapanen, J. Harra, C. Stenroos, J. Lahti, J. Kuusipalo, J.M. Mäkelä, P. Vuoristo, Icephobicity of slippery liquid infused porous surfaces under multiple freeze-thaw and ice accretion-detachment cycles, Adv. Mater. Interfaces 5 (2018), 1800828, https://doi.org/10.1002/admi.201800828.
[25] S. Ozbay, C. Yuceel, H.Y. Erbil, Improved icephobic properties on surfaces with a hydrophilic lubricating liquid, ACS Appl. Mater. Interfaces 7 (2015) 22067–22077, https://doi.org/10.1021/acsami.5b07265.
[26] H.Y. Erbil, Improvement of lubricant-infused surfaces for anti-icing applications, Surf. Innov. 4 (2016) 214–217, https://doi.org/10.1680/jsuin.16.00026.
[27] S.B. Subramanyam, K. Rykaczewski, K.K. Varanasi, Ice adhesion on lubricant-impregnated textured surfaces, Langmuir 29 (2013) 13414–13418, https://doi.org/10.1021/la402456c.
[28] S. Ozbay, H.Y. Erbil, Ice accretion by spraying supercooled droplets is not dependent on wettability and surface free energy of substrates, Colloids Surfaces A Physicochem. Eng. Asp. 504 (2016) 210–218, https://doi.org/10.1016/j.colsurfa.2016.05.065.
[29] H. Koivuluoto, E. Hartikainen, H. Niemelä-Anttonen, Thermally sprayed coatings: novel surface engineering strategy towards icephobic solutions, Materials 13 (2020), https://doi.org/10.3390/ma13061434. Basel.
[30] A.J. Meuler, J.D. Smith, K.K. Varanasi, J.M. Mabry, G.H. McKinley, R.E. Cohen, Relationships between water wettability and ice adhesion, ACS Appl. Mater. Interfaces 2 (2010) 3100–3110, https://doi.org/10.1021/am1006035.
[31] Z. He, E.T. Vågenes, C. Delabahan, J. He, Z. Zhang, Room temperature characteristics of polymer-based low ice adhesion surfaces, Sci. Rep. 7 (2017) 1–7, https://doi.org/10.1038/srep42181.
[32] H. Koivuluoto, C. Stenroos, M. Kylmälahti, M. Apostol, J. Kiilakoski, P. Vuoristo, Anti-icing behavior of thermally sprayed polymer coatings, J. Therm. Spray Technol. 26 (2017) 150–160, https://doi.org/10.1007/s11666-016-0501-x.
[33] V. Donadei, H. Koivuluoto, E. Sarlin, P. Vuoristo, Icephobic behaviour and thermal stability of flame-sprayed polyethylene coating: the effect of process parameters, J. Therm. Spray Technol. 29 (2020) 241–254, https://doi.org/10.1007/s11666-019-00947-0.
[34] Y. Zhuo, V. Håkonsen, Z. He, S. Xiao, J. He, Z. Zhang, Enhancing the mechanical durability of icephobic surfaces by Introducing autonomous self-healing function, ACS Appl. Mater. Interfaces 10 (2018) 11972–11978, https://doi.org/10.1021/acsami.8b01866.
[35] H. Memon, D.S.A. De Focatiis, K.S. Choi, X. Hou, Durability enhancement of low ice adhesion polymeric coatings, Prog. Org. Coat. 151 (2021) 106033, https://doi.org/10.1016/j.porgcoat.2020.106033.
[36] S.A. Kulinich, D. Masson, X. Du, A.M. Emelyanenko, K.L. Mittal, C.-H. Choi, Testing the durability of anti-icing coatings, in: Ice Adhes. Mech. Meas. Mitig, Wiley, 2020, pp. 495–520, https://doi.org/10.1002/9781119640523.ch16.
[37] V. Donadei, H. Koivuluoto, E. Sarlin, P. Vuoristo, Lubricated icephobic coatings prepared by flame spraying with hybrid feedstock injection, Surf. Coat. Technol. 403 (2020), 126396, https://doi.org/10.1016/j.surfcoat.2020.126396.
[38] V. Jannin, Y. Cuppok, Hot-melt coating with lipid excipients, Int. J. Pharm. 457 (2013) 480–487, https://doi.org/10.1016/j.ijpharm.2012.10.026.
[39] A. Sandhu, O.J. Walker, A. Nistal, K.L. Choy, A.J. Clancy, Perfluoroalkane wax infused gels for effective, regenerating, anti-icing surfaces, Chem. Commun. 55 (2019) 3215–3218, https://doi.org/10.1039/c8cc09818b.
[40] H. Koivuluoto, C. Stenroos, R. Ruohomaa, G. Bolelli, L. Lusvarghi, P. Vuoristo, Research on icing behavior and ice adhesion testing of icephobic surfaces, in: Proc. Int. Work. Atmos. Icing Struct., Uppsala, 2015, pp. 183–188.
[41] C. Stenroos, P. Vuoristo, H. Koivuluoto, Properties of Icephobic Surfaces in Different Icing Conditions, Mater Thesis, Tampere University of Technology, Tampere, FI, 2015.
[42] H. Niemelä-Anttonen, J. Kiilakoski, P. Vuoristo, H. Koivuluoto, Icephobic performance of different surface designs and materials, Proc. Int. Work. Atmos. Icing Struct. (2019) 1–5.
[43] ISO 25178-3:2012 - Geometrical product specifications (GPS) — Surface texture: Areal — Part 3: Specification operators. https://www.iso.org/standard/42895.html, 2012. (Accessed 6 February 2020).
[44] ISO 25178-2:2012 - Geometrical product specifications (GPS) — Surface texture: Areal — Part 2: Terms, definitions and surface texture parameters. https://www.iso.org/standard/42785.html, 2012. (Accessed 27 May 2021).
[45] S. Rønneberg, Y. Zhuo, C. Laforte, J. He, Z. Zhang, Interlaboratory study of ice adhesion using different techniques, Coatings 9 (2019) 678, https://doi.org/10.3390/coatings9100678.
[46] S. Asadollahi, M. Farzaneh, L. Stafford, On the icephobic behavior of organosilicon-based surface structures developed through atmospheric pressure plasma deposition in nitrogen plasma, Coatings 9 (2019) 679, https://doi.org/10.3390/coatings9100679.
[47] S. Rønneberg, J. He, Z. Zhang, The need for standards in low ice adhesion surface research: a critical review, J. Adhes. Sci. Technol. 34 (2020) 319–347, https://doi.org/10.1080/01694243.2019.1679523.
[48] A. Work, Y. Lian, A critical review of the measurement of ice adhesion to solid substrates, Prog. Aerosp. Sci. 98 (2018) 1–26, https://doi.org/10.1016/j.paerosci.2018.03.001.
[49] P. Eberle, M.K. Tiwari, T. Maitra, D. Poulikakos, Rational nanostructuring of surfaces for extraordinary icephobicity, Nanoscale 6 (2014) 4874–4881, https://doi.org/10.1039/c3nr06644d.
[50] J. Chen, J. Liu, M. He, K. Li, D. Cui, Q. Zhang, X. Zeng, Y. Zhang, J. Wang, Y. Song, Superhydrophobic surfaces cannot reduce ice adhesion, Appl. Phys. Lett. 101 (2012) 111603, https://doi.org/10.1063/1.4752436.
[51] M. Balordi, G. Santucci de Magistris, C. Chemelli, A novel simple anti-ice aluminum coating: synthesis and in-lab comparison with a superhydrophobic hierarchical surface, Coatings 10 (2020) 111, https://doi.org/10.3390/coatings10020111.
[52] L.B. Boinovich, E.B. Modin, A.R. Sayfutdinova, K.A. Emelyanenko, A.L. Vasiliev, A. M. Emelyanenko, Combination of functional nanoengineering and nanosecond laser texturing for design of superhydrophobic aluminum alloy with exceptional mechanical and chemical properties, ACS Nano 11 (2017) 10113–10123, https://doi.org/10.1021/acsnano.7b04634.
[53] L.B. Boinovich, A.M. Emelyanenko, V.K. Ivanov, A.S. Pashinin, Durable icephobic coating for stainless steel, ACS Appl. Mater. Interfaces 5 (2013) 2549–2554, https://doi.org/10.1021/am3031272.
[54] L. Makkonen, Ice adhesion - theory, measurements and countermeasures, J. Adhes. Sci. Technol. 26 (2012) 413–445, https://doi.org/10.1163/016942411X574583.
[55] J.H. Kim, M.J. Kim, B. Lee, J.M. Chun, V. Patil, Y.S. Kim, Durable ice-lubricating surfaces based on polydimethylsiloxane embedded silicone oil infused silica aerogel, Appl. Surf. Sci. 512 (2020) 145728, https://doi.org/10.1016/j.apsusc.2020.145728.
[56] S. Brown, J. Lengaigne, N. Sharifi, M. Pugh, C. Moreau, A. Dolatabadi, L. Martinu, J.E. Klemberg-Sapieha, Durability of superhydrophobic duplex coating systems for aerospace applications, Surf. Coat. Technol. 401 (2020), https://doi.org/10.1016/j.surfcoat.2020.126249.
[57] Z.A. Janjua, B. Turnbull, K.L. Choy, C. Pandis, J. Liu, X. Hou, K.S. Choi, Performance and durability tests of smart icephobic coatings to reduce ice adhesion, Appl. Surf. Sci. 407 (2017) 555–564, https://doi.org/10.1016/j.apsusc.2017.02.206.
[58] V. Vercillo, J.T. Cardoso, D. Huerta-Murillo, S. Tonnicchia, A. Laroche, J.A. Mayén Guillén, J.L. Ocaña, A.F. Lasagni, E. Bonaccurso, Durability of superhydrophobic laser-treated metal surfaces under icing conditions, Mater. Lett. X. 3 (2019), 100021, https://doi.org/10.1016/j.mlblux.2019.100021.
[59] V. Donadei, H. Koivuluoto, E. Sarlin, P. Vuoristo, Durability of lubricated icephobic coatings under multiple icing/deicing cycles, in: F. Azarmi, X. Chen, J. Cizek, C. Cojocaru, B. Jodoin, H. Koivuluoto, Y. Lau, R. Fernandez, O. Ozdemir, H. Salami Jazi, F.L. Toma (Eds.), Proc. from Int. Therm. Spray Conf, ASM International, Anaheim, CA, USA, Quebec City, 2021, pp. 473–481, https://doi.org/10.31399/asm.cp.itsc2021p0473.
[60] S.A. Kulinich, M. Farzaneh, On ice-releasing properties of rough hydrophobic coatings, Cold Reg. Sci. Technol. 65 (2011) 60–64, https://doi.org/10.1016/j.coldregions.2010.01.001.
[61] A. Laroche, D. Bottone, S. Seeger, E. Bonaccurso, Silicone nanofilaments grown on aircraft alloys for low ice adhesion, Surf. Coat. Technol. 410 (2021) 126971, https://doi.org/10.1016/j.surfcoat.2021.126971.
[62] N. Rehfeld, B. Speckmann, C. Schreiner, V. Stenzel, Assessment of icephobic coatings—how can we monitor performance durability? Coatings 11 (2021) 614, https://doi.org/10.3390/coatings11060614.

[63] Q. Fu, X. Wu, D. Kumar, J.W.C. Ho, P.D. Kanhere, N. Srikanth, E. Liu, P. Wilson, Z. Chen, Development of sol-gel icephobic coatings: effect of surface roughness and surface energy, ACS Appl. Mater. Interfaces 6 (2014) 20685–20692, https://doi.org/10.1021/am504348x.
[64] L. Mazzola, G. Bruno, Characterization of ice-phobic surfaces: improvements on contact angle measurements, Measurement 110 (2017) 202–210, https://doi.org/10.1016/j.measurement.2017.06.036.
[65] D. Quéré, Wetting and roughness, Annu. Rev. Mater. Res. 38 (2008) 71–99, https://doi.org/10.1146/annurev.matsci.38.060407.132434.
[66] E. Shafrin, W. Zisman, Upper limits to the contact angles of liquids on solids, in: R. F. Gou (Ed.), Contact Angle, Wettability Adhes. Adv. Chem. Ser, DC: Am. Chem. Soc., Washington, 1964, pp. 478–479, https://doi.org/10.1007/bf01150624.
[67] A. Lafuma, D. Quéré, Superhydrophobic states, Nat. Mater. 2 (2003) 457–460, https://doi.org/10.1038/nmat924.
[68] G. Momen, M. Farzaneh, R. Jafari, Wettability behaviour of RTV silicone rubber coated on nanostructured aluminium surface, Appl. Surf. Sci. 257 (2011) 6489–6493, https://doi.org/10.1016/j.apsusc.2011.02.049.
[69] T. Mouterde, G. Lehoucq, S. Xavier, A. Checco, C.T. Black, A. Rahman, T. Midavaine, C. Clanet, D. Quéré, Antifogging abilities of model nanotextures, Nat. Mater. 16 (2017) 658–663, https://doi.org/10.1038/nmat4868.
[70] A. Hakimian, S. Nazifi, H. Ghasemi, Durability assessment of icephobic coatings, in: Ice Adhes. Mech. Meas. Mitig, Wiley, 2020, pp. 521–545, https://doi.org/10.1002/9781119640523.ch17.
[71] A.A. Abubakar, A.F.M. Arif, K.S. Al-Athel, S.S. Akhtar, J. Mostaghimi, Modeling residual stress development in thermal spray coatings: current status and way forward, J. Therm. Spray Technol. 26 (2017) 1115–1145, https://doi.org/10.1007/s11666-017-0590-1.
[72] G. Montay, A. Cherouat, A. Nussair, J. Lu, Residual stresses in coating technology, J. Mater. Sci. Technol. 20 (2004) 81–84.
[73] M.E. Nichols, C.A. Darr, C.A. Smith, M.D. Thouless, E.R. Fischer, Fracture energy of automotive clearcoats - I. Experimental methods and mechanics, Polym. Degrad. Stab. 60 (1998) 291–299, https://doi.org/10.1016/s0141-3910(97)00081-5.